Environ Monit Assess (2025) 197:244
https://doi.org/10.1007/s10661-025-13674-7

RESEARCH

Metabolomic profiling of paper board sludge biochar for agricultural use

T. Sherene Jenita Rajammal · Vaishnavi Pandurangan · Baskar Murugaiyan · Vanniarajan Chockalingam · S. A. Ramjani

Received: 18 September 2024 / Accepted: 24 January 2025

Abstract The pulp and paperboard industries are the major industrial sector that consumes significant amounts of fresh water and generates large volumes of wastewater. The treatment of this wastewater resulted in the production of a substantial amount of sludge, which posed serious environmental challenges. This study explored a sustainable solution by converting PBS into biochar through slow pyrolysis of temperatures up to ≤ 500 °C, offering an alternative approach to waste management and resource conservation. The physicochemical parameters of paper board sludge biochar (PBSB) exhibited a neutral pH of 7.49, electrical conductivity of 0.09 dS m^{-1}, organic carbon of 38.12% and $CaCO_3$ of 24.5%. Proximate analysis of PBSB revealed an increased fixed carbon of 76.43%, total organic carbon (TOC) of 7.13%, and reduced volatile matter and moisture levels. The TGA analysis of the dried paperboard sludge sample showed a 20% mass reduction when heated to 350 °C. During this process, more than 90% of the volatile components were removed.. The micro nutrients viz., Fe 5.06 mg L^{-1}, Mn 419.3 mg L^{-1}, Cu 26.3 mg L^{-1}, and Zn 66.1 mg L^{-1} contents were observed in PBSB. FT-IR analysis identified the presence of various carbon-containing functional groups, including C–Cl, C–N, C–C, H–C = O, C–H, and –C≡C–H, indicating substantial chemical transformations during pyrolysis. SEM–EDX analysis revealed that PBSB has fine particle size and a coarse fluffy spongy porous structure ideal for water adsorption. Elemental analysis (XRD) showed high carbon and oxygen content with significant amounts of aluminosilicates, carbonates, and nutrients like phosphorus and potassium, suggesting PBSB as a potential slow-release fertilizer. This research highlights the potential of biochar derived from paperboard waste as a sustainable solution for waste management and resource recovery.

Keywords Biochar · Physicochemical and proximate analysis · PBS · Functional groups · Surface and elemental analysis

T. S. J. Rajammal · V. Pandurangan (✉) · B. Murugaiyan
Department of Soil Science and Agricultural Chemistry, Anbil Dharmalingam Agricultural College and Research Institute, Tamil Nadu Agricultural University, Coimbatore 641003, India
e-mail: vaishnavip3152001@gmail.com

T. S. J. Rajammal
e-mail: shereneraj@yahoo.co.in

B. Murugaiyan
e-mail: mbaskaruma@gmail.com

V. Chockalingam
Department of Genetics and Plant Breeding, Anbil Dharmalingam Agricultural College and Research Institute, Tamil Nadu Agricultural University, Coimbatore 641003, India
e-mail: deanagritry@tnau.ac.in

S. A. Ramjani
Department of Renewable Energy Engineering, Agricultural Engineering College and Research Institute, Tamil Nadu Agricultural University, Coimbatore, India
e-mail: ramjani.sa@tnau.ac.in

Published online: 05 February 2025

Introduction

In India, the pulp and paperboard industries are significant consumer of water, with each tonne of paper generating 72 to 225 m^3 of wastewater, depending on the production method used (Jaria et al., 2017). This large amount of wastewater must be treated to meet environmental quality standards before reusing it. The effluent treatment in the pulp and paperboard industry generates a substantial amount of sludge, creating a significant environmental burden (Tawalbeh et al., 2021). One tonne of paper typically produces 40–50 kg of dry sludge (Bajpai, 2015). One of the main challenges in the paperboard industry is waste management, due to increasingly stringent environmental requirements (Jaria et al., 2017). Efficient solutions need to consider both environmental and economic factors. Previously disposing of sludge in a landfill has been the accepted method (Likon and Trebše, 2012).

The waste of the paperboard industry can be repurposed as raw materials for various applications, so it is imperative to establish sustainable processes. In the past two decades, researchers have explored innovative approaches to repurpose waste from the paperboard industry into valuable materials. PBS can be used as a dried formulation for agricultural fertilizers, building materials, insulation materials, etc., as reported by Likon and Trebše (2012). Some researchers have reported that because of its high carbon content, PBS can be used to produce activated carbon, which can be applied to soil to enhance the carbon content (Ferreira et al., 2016). This conversion method not only increases soil carbon content but also addresses environmental issues related to waste disposal and conserves natural resources. This study aims to evaluate the uniformity of carbon-rich biochar derived from pyrolyzing paper board sludge. The research assesses the physical and chemical properties of the resulting materials and examines how different input components influence them to determine their potential applications. Thermogravimetric analysis (TGA), Fourier transform infrared spectroscopy (FT-IR), scanning electron microscopy with energy dispersive X-ray spectroscopy (SEM–EDX), X-ray diffraction (XRD), proximate analysis, and comprehensive physicochemical analysis were employed to characterize both raw paper board sludge and the resulting biochar.

Materials and methods

Study area

The research area is situated in Mondipatti Village, Manaparai Taluk, Tiruchirappalli district, Tamil Nadu, at Tamil Nadu Newsprint and Paper Limited (TNPL)-Unit II. This plant uses waste paper and imported pulp as raw materials to produce multilayer coated paper boards. Located at the junction of latitude and longitude roughly 10° 41′ N and 78° 26′ E, the facility can produce approximately 200,000 tons of product annually and treats approximately 5000 m^3 of effluent per day using a modernized effluent treatment plant (ETP).

Sample collection

PBS was obtained from the recycled paper industry of ETP at TNPL Unit-II, Mondipatti, Tiruchirappalli, Tamil Nadu. These solid wastes were generated during the effluent treatment process. The raw paper board sludge was collected in polyethylene bags and shade-dried for further analysis.

Biochar production

Slow pyrolysis process

Pyrolysis is a commonly employed method for the thermal conversion of biomass. In this study, the slow pyrolysis technique is used to process PBS into biochar. This method involves thermally treating biomass in an environment with limited or no oxygen, a process known as slow pyrolysis (Manyà, 2012). A pyrolizer with a 10 kg capacity is used for biochar production. Slow pyrolysis, characterized by a heating rate of approximately 0.1–1 °C per second, results in a higher yield of char. During the slow pyrolysis of wood, the biomass is heated to around 500 °C, characterized. The pyrolysis process transforms PBS into valuable carbon-rich biochar (Figs. 1, 2). After pyrolysis, the pyrolyzed PBSB is cooled and ground into a powder, and it is suitable for soil application, water filtration, and carbon sequestration (Jaria et al., 2017).

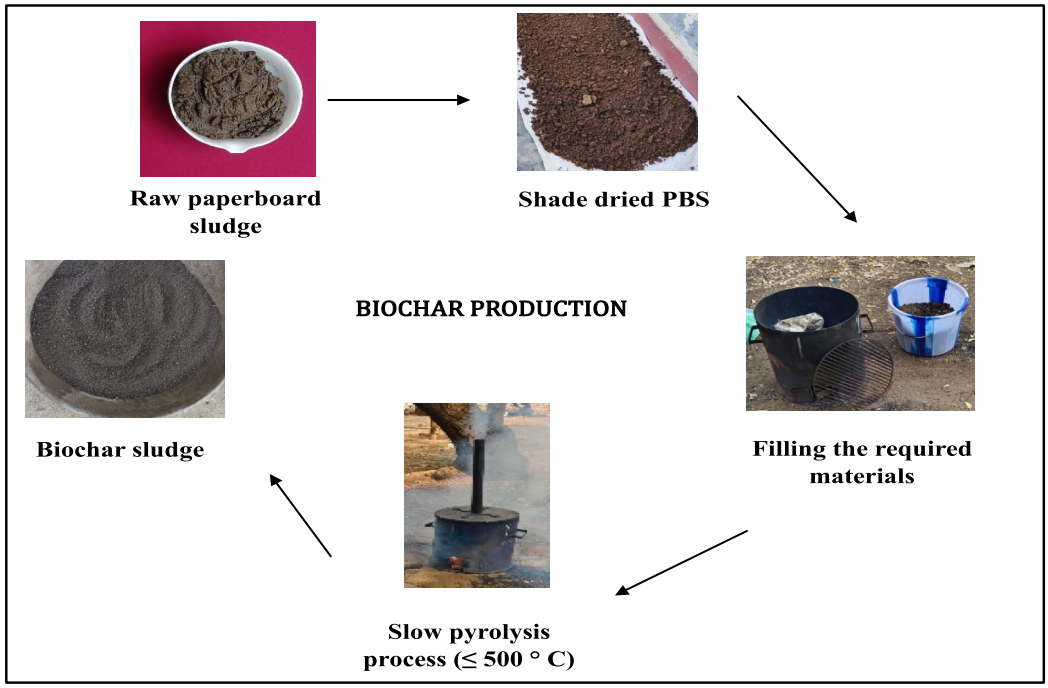

Fig. 1 Biochar production through a slow pyrolysis process

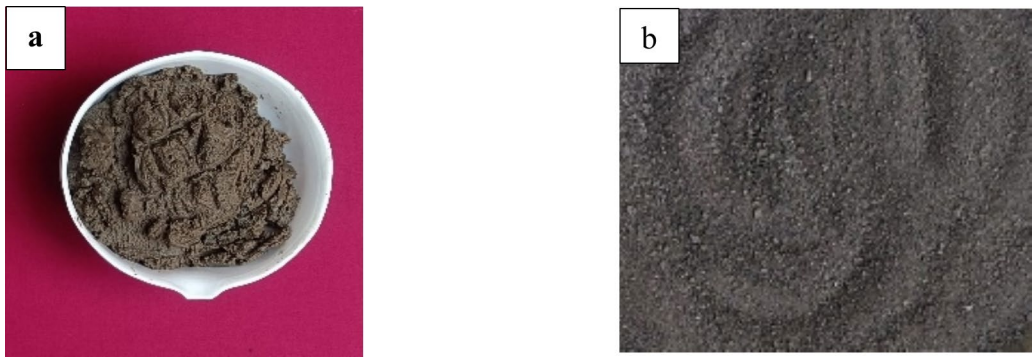

Fig. 2 Visual observation of **a** PBS and **b** PBSB

Physicochemical analysis of PBS and PBSB

All the physicochemical parameters were measured according to the standard methods (Jackson 1973). This study considered the physicochemical parameters of pH, electrical conductivity (EC), organic carbon (OC), total nitrogen, total phosphorus, total potassium, total calcium, total magnesium, and $CaCO_3$ content using HCl and measuring the evolved CO_2. Micronutrients (Cu, Fe, Mn, Zn) were analyzed in an atomic absorption spectrophotometer (Thermo Electron; Model IRIS Intrepid IIXDL, iCe 3000 series USA).

Proximate analysis for PBS and PBSB

The proximate analysis provides information regarding the moisture content, volatile matter content, ash content, and fixed carbon content of PBS and PBSB.

Moisture content

The moisture content of a PBS and PBSB sample is determined by heating it just above the boiling point of water (105 °C). This process causes the water in the PBS and PBSB to evaporate, changing its weight. When the weight remains constant, the difference between the initial and final weights indicates the moisture content, which is expressed as a percentage of the PBS and PBSB (Agrafioti et al., 2013; ASTM, 2005). The percentage of moisture content was determined as follows in Eq. (1):

$$\textit{Moisture content}\ (\%) = \frac{W_{1-W_2}}{W_1} \times 100 \tag{1}$$

where W_1 is the initial weight of sample (g), and W_2 is the final weight of sample (g).

Volatile matter

The volatile matter was determined according to the standard methods of APHA (1926). A dried sample of PBS and PBSB was placed in a pre-weighed crucible and heated in a muffle furnace at 900 °C for 1 h in a non-oxidizing atmosphere after that cooled in a desiccator and weighed. Heating was repeated for 30 min each time until a constant weight was obtained. The percentage of volatile matter was determined as follows in Eq. (2):

$$\textit{Volatile matter}\ (\%) = \frac{M_{f-V_f}}{M_f} \times 100 \tag{2}$$

where M_f is the final weight of moisture content, and V_f is the final weight of volatile matter.

Ash content

To determine the ash content of the PBS and PBSB, the dried samples and crucible were weighed together and then heated in a muffle furnace at 750 °C for 1 h. After cooling in a desiccator, the crucible and ash were weighed (Agrafioti et al., 2013). The percentage of ash content was determined as follows in Eq. (3):

$$\text{Ashcontent}\ (\%) = \frac{\text{Weight of ash formed (g)}}{\text{Weight of dried sample (g)}} \times 100 \tag{3}$$

Fixed carbon

When the moisture content (%), ash content (%), and volatile matter (%) are removed from the PBS and PBSB, the remaining is the fixed carbon, as shown in Eq. (4) (Agrafioti et al., 2013).

$$\textit{Fixed carbon}\ (\%) = 100 - (\%MC + \%Ash + \%VM) \tag{4}$$

Total organic carbon (TOC)

Dry the sample at a temperature of 105 °C to constant weight. Weigh the dried sample and place the sample in a pre-weighed porcelain crucible. Heat the crucible with the sample to 550–600 °C in a muffle furnace for about 4 h. After 4 h, cool the crucible, weigh it, and calculate the weight loss as the difference between the weight of the crucible with the soil sample before and after ignition. These weights represent the amount of total organic carbon in the sample (Jaria et al., 2017). The equation is shown in (5).

$$TOC\ (\%) = (\textit{Weight loss upon ignition}/\ \textit{initial weight of the sample}) \times 100 \tag{5}$$

(Weight loss upon ignition = Initial weight of sample – Weight of crucible with residue after ignition).

Fourier transform infrared spectrometer (FT-IR)

FT-IR results were recorded by using the Fourier transform infrared spectrometer (FT-IR) model PerkinElmer Spectrum II spectrometer using KBr pellets. The sample was dried, powdered, and sieved in a 2-mm sieve. The homogeneous mixture of PBS was prepared with a motor and pestle before analyzing FT-IR. Samples were directly placed into the sample container, and data were collected from 4000 to 400 cm^{-1} using 21 CFR part 11 software. Reference spectra were obtained before each sample analysis. Peak values were recorded, and each analysis was repeated twice for confirmation (Méndez et al., 2009).

Scanning electron microscope–energy dispersive X-ray spectroscopy (SEM–EDX)

For scanning electron microscopy, 10 mg PBS and PBSB were spotted on high-purity aluminum stubs.

These were left to air dry at 37 °C before being coated under a vacuum with approximately 25 nm of high-purity platinum. The samples were placed on an aluminum stub and coated with platinum using a sputter coater. For elemental analysis of the PBS and PBSB, an area was selected, and the elements in the sediment were examined by a high-resolution scanning electron microscope equipped with an EDAX system (Méndez et al., 2009).

X-ray diffraction analyzer (XRD)

XRD experiments were performed with a PANalytical empyrean diffractometer (PANalytical Expert TERP) equipped with a Cu X-ray source ($k = 1.5404$ Å) operated at 45 kV and 30 mA. The prepared samples were placed on a quartz holder for analysis. Each diffractogram was measured at 2θ and 0.05° intervals, in the range of 5–90° (Tawalbeh et al., 2021).

Thermogravimetric analysis (TGA)

Thermal gravimetric analysis (TGA) is a method of thermal analysis in which changes in physical and chemical properties of materials are measured as a function of increasing temperature (with constant heating rate), or as a function of time (with constant temperature and/or constant mass loss. Thermal gravimetric analysis (TGA) is a technique used to study the thermal decomposition of raw paperboard sludge with long-term stability indicate high oxidation resistance. Thermogravimetric analysis (TGA) was adopted to determine the oxidation resistance of raw paperboard sludge in this study (Yang et al., 2016). Nitrogen is used as carrier gas at 30 ml/min in TGA. Through this analysis we can obtain information about thermal behavior, energy activation and ash content, and the decomposition of gaseous products can be identified.

Results and discussion

Physicochemical properties of PBS and PBSB

The comparative analysis of the physicochemical properties of PBS and PBSB is shown in Table 1. The pH of PBS was acidic at 6.84 and PBSB was neutral at 7.49. The electrical conductivity of the PBS was 2.43 dS m^{-1}, and the electrical conductivity of the PBSB was 0.90 dS m^{-1}. These findings align with the research of Faubert et al. (2016); Oumabady et al. (2020); Guo (2020); and Sabarish et al. (2021). The slightly acidic pH of the PBS (6.84) may be attributed to the low concentration of calcium carbonate ($CaCO_3$), which is insufficient to neutralize the acidity present in the material. Reduced levels of $CaCO_3$ were associated with lower pH levels as noted in the study by (Méndez et al., 2009). PBSB has a neutral pH of 7.49. Due to being produced at lower temperatures (≤ 500 °C), it leads to neutral conditions. Neutral to the alkaline condition of biochar pH was due to the higher $CaCO_3$ content as noted by Guo (2020); Sabarish et al. (2021); Venkatesh et al. (2022); and Junior and Guo (2023). PBS shows low organic carbon 24.30% compared to PBSB 38.12%. The low amount of organic carbon in PBS was due to a high cellulose fiber content as noted by Nelson and Sommers (1982); (Méndez et al., 2009); and Kambo and Dutta (2015). The organic carbon content of biochar is dependent on the feedstock and pyrolyzing conditions. The organic carbon in biochar largely forms polyaromatic structures. According to Guo (2020), pyrolysis promotes the formation of aromatic rings that are resistant to microbial degradation resulting in a more stable carbon content in biochar. This stable aromatic carbon is a key reason for the increased organic carbon in biochar. The pyrolysis leads to the

Table 1 Physicochemical parameters of PBS and PBSB

S. No	Parameters	Unit	PBS	PBSB
1.	pH	-	6.84	7.49
2.	EC	dS m^{-1}	2.43	0.09
3.	Organic carbon	%	24.30	38.12
4.	C:N ratio	-	13.96	29.78
5.	CEC	C mol (p^+) kg^{-1}	2.50	5.00
6.	$CaCO_3$	%	7.00	24.5
7.	Total nitrogen	%	1.74	1.28
8.	Total phosphorus	%	0.58	0.24
9.	Total potassium	%	0.84	0.38
10.	Total calcium	%	4.39	2.37
11.	Total magnesium	%	2.36	0.57
12.	Zinc	mg L^{-1}	95.82	66.08
13.	Copper	mg L^{-1}	32.16	26.34
14.	Iron	mg L^{-1}	1607.92	5.06
15.	Manganese	mg L^{-1}	532.78	419.34

loss of volatile organic compounds, with non-carbon elements like oxygen and hydrogen being produced. This results in a higher concentration of carbon in biochar. Due to the decreased mass of other components, it stabilizes the carbon and increases the organic carbon in biochar as reported by Lehmann and Joseph (2015). The C:N ratio of PBS was 13.9 and PBSB was 29.78 which aligns with the findings of Faubert et al. (2016). The total nitrogen, total phosphorus, total potassium, total calcium, and total magnesium content of PBS was 1.74%, 0.58%, 0.84%, 4.39%, and 2.36% and PBSB was 1.28%, 0.24%, 0.38%, 2.37%, and 0.57% respectively which it aligns with findings of Faubert et al. (2016) and Turner et al. (2022). The total Ca^{2+}, Mg^{2+}, and K^{+} content of the PBS was high compared to PBSB due to the paper produced from virgin wood materials as reported by Méndez et al. (2009). The $CaCO_3$ content of PBS was 7.00%, and the $CaCO_3$ content of PBSB was 24.5%. PBS biochar shows higher $CaCO_3$ levels, and PBS has lower $CaCO_3$ due to the removal of inorganic fillers from recycled paper (Nelson and Sommers, 1982). PBS has a lower amount of cation exchange capacity of 2.5 C mol (p^{+}) kg^{-1} than PBSB as 5.00 C mol (p^{+}) kg^{-1}. The low amount of CEC depends on organic matter and clay content it varies as reported by Turner et al. (2022). The CEC of biochar indicates its capability to retain exchangeable cations through the sorption pathway as reported by Holladay et al. (2007). The micronutrients, viz. zinc, copper, iron, and manganese of PBS were 95.82 mg L^{-1}, 32.16 mg L^{-1}, 1607.92 mg L^{-1}, and 532.78 mg L^{-1}, and PBSB was 66.08 mg L^{-1}, 26.34 mg L^{-1}, 5.06 mg L^{-1}, and 419.34 mg L^{-1}.

Proximate analysis for PBS and PBSB

The proximate analysis of PBS and PBSB is shown in Table 2. The moisture content of PBS was 40.17% and PBSB was 0.55%. The ash content in PBSB was 12.13%, while PBS has an ash content of 11.75%. The findings align with the studies of Agrafioti et al. (2013); Oumabady et al. (2020); Sabarish et al. (2021); and Junior and Guo (2023). The volatile matter in PBS is 35.29%, compared with PBSB at 10.89% due to the organic matter content the volatile matter differs from PBS and PBSB (Méndez et al., 2009). For PBSB, the volatile matter varies according to the temperature (Hossain et al., 2011). The fixed carbon content of PBS was 12.79% and the PBSB was 76.43%. The PBSB has significantly increased fixed carbon content compared with PBS. The total organic carbon for PBS was 1.03% and PBSB was 7.13%, which aligns with the findings of (Jaria et al., 2017).

Table 2 Proximate analyses and total organic carbon (TOC) for PBS and PBSB

S. No	Parameter	Unit	PBS	PBSB
1.	Moisture	%	40.17	0.55
2.	Ash	%	11.75	12.13
3.	Volatile matter	%	35.29	10.89
4.	Fixed carbon	%	12.79	76.43
5.	Total organic carbon (TOC)	%	1.03	7.13

Thermogravimetric analysis (TGA)

The thermal behavior of the raw PBS was analyzed using thermogravimetric analysis (TGA) under an air atmosphere. TGA also gives the upper use temperature of a material. Beyond this temperature, the material will begin to degrade. The mass loss observed between 39.23 and 193.69 °C was approximately 7.108%, corresponding to a weight loss of 0.788 mg, which can be attributed to the evaporation of physically bound water and the release of light volatile compounds. This initial phase is consistent with the findings of Yang et al. (2016), who reported similar mass losses during the dehydration of organic materials such as paperboard sludge at low temperatures.

Between 193.36 and 400.18 °C, a more significant weight loss of 13.878% (1.538 mg) was recorded, indicating the thermal degradation of organic components such as hemicellulose, cellulose, and other volatile organic compounds present in the raw paperboard sludge. This phase aligns with the findings of Harvey et al. (2012), who observed that organic residues typically undergo major degradation in this temperature range due to the decomposition of labile carbon fractions. The use of an air atmosphere further facilitated oxidation, contributing to the breakdown of less stable organic structures during this phase. The TGA analysis is carried out for the raw PBS sample observed that 7% of mass reduction was observed upto the temperature level of 150 ℃. Further, there is

a mass reduction of 17% observed for the temperature level upto 350 ℃. In total, there is a 20% mass reduction for the dried paperboard sludge sample. Hence, within 350 ℃, more than 90% of the volatiles can be removed as shown in Fig. 3. The heat flow curve is shown in Fig. 4.

Functional groups identified for PBS and PBSB

The functional groups of PBS and PBSB are shown in Table 3. The functional groups in the PBS such as = C–H (methine group), C–C (alkene group), N–H (primary amine group), C = O (carbonyl group), H–C = O (carboxyl group), and C–H were observed (Fig. 5). The broad band at 870 cm^{-1} in PBS may indicate the presence of $CaCO_3$ and corresponds to significant C-H stretching in aromatic groups. In PBS C–H bond absorption may be due to the mulling oil usage in paper production. The peak at 995.53 cm^{-1} may be attributed to the bending vibrations of methylene or alkene groups = C–H with strong intensity. These = C–H methine or alkene groups, representing alkenes or unsaturated hydrocarbons, could arise from the breakdown of resin acids, unsaturated fatty acids, or other organic compounds in the wood or recycled fibers used in paperboard production as reported by Holladay et al. (2007). The peak at 1406.27 cm^{-1} may correspond to C–C stretching in aromatic groups with medium intensity. The broadband at 1628.41 cm^{-1} may be associated with the N–H bending vibrations of primary amines (asymmetric stretching), which may suggest a partial breakdown of nitrogenous compounds that results in the formation of amide or amine functional groups in the PBS. These groups could enhance the nutrient content of the PBS (Bolan et al., 2012). The peak at 1779.94 cm^{-1} may correspond to C = O (carbonyl group) stretching in anhydrides, which may be formed from the oxidation of organic materials during the papermaking process (Greyer et al. 2017; Tawalbeh et al., 2021). A medium-intensity peak at 2794.01 cm^{-1} may attributed to the C-H stretching in aldehyde groups, specifically related to the carbonyl stretching of H–C = O, while the peak at 2882.67 cm^{-1} may correspond to the C–H stretching suggesting the presence of saturated hydrocarbons (alkanes). PBS has C–H adsorptions due to the mulling oil. Mulling oil is utilized in the paperboard industry to enhance the final product. It is used for several purposes, including improving the coating, mixing with pigments, and other additives added together for uniform coating; it also enhances ink absorption and better print quality as reported by Kumar and Chopra (2015);

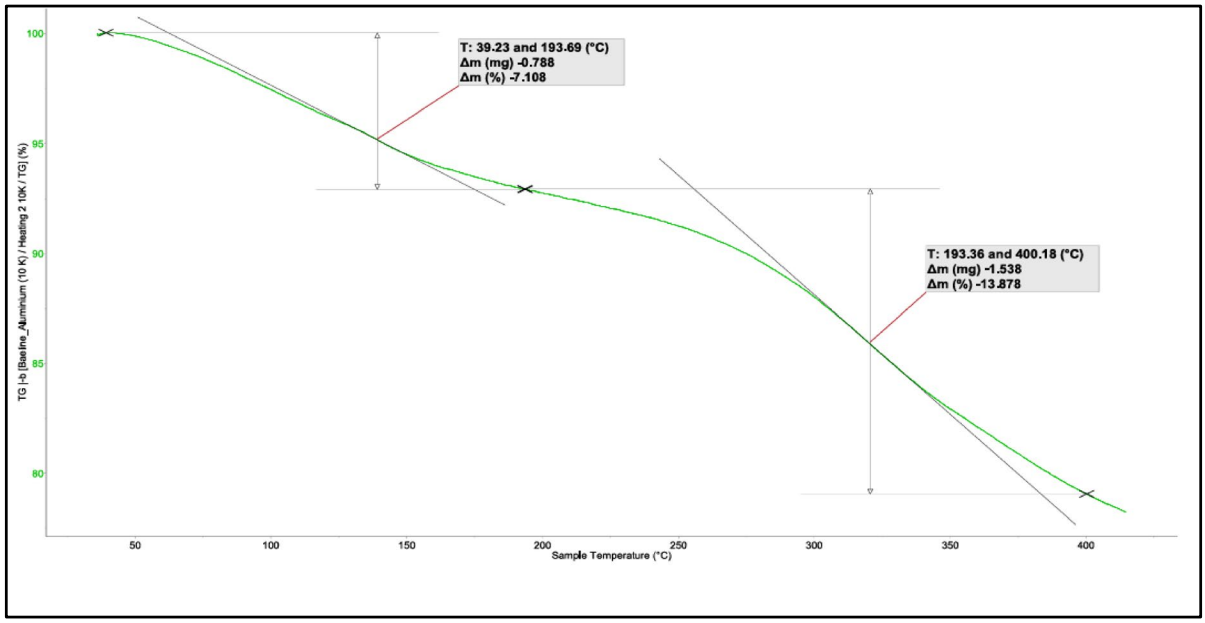

Fig. 3 Thermogravimetric analysis of raw paperboard sludge

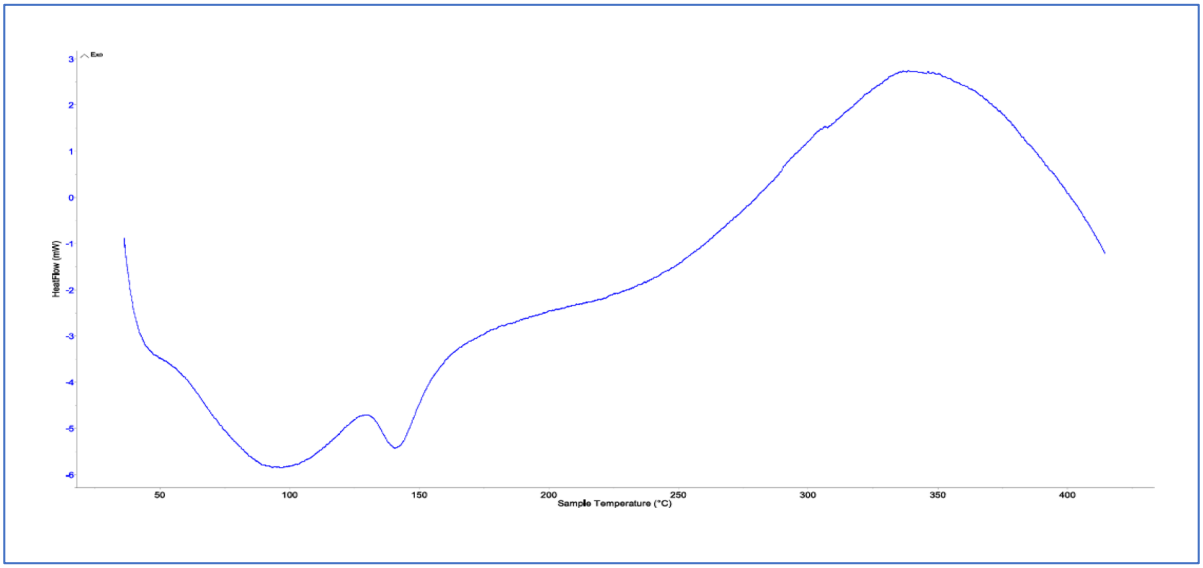

Fig. 4 Heat flow curve of raw paperboard sludge

Table 3 Summary of identified FT-IR band observed in PBS and PBSB

PBS				PBSB			
Peak value (cm^{-1})	**Nature of band stretching (cm^{-1})**	**Functional group**	**Intensity**	**Peak value (cm^{-1})**	**Nature of band stretching (cm^{-1})**	**Functional group**	**Intensity**
870	C–H bend	Aromatics	Strong	850	C–Cl stretching	Alkyl halides	Medium
995.53	(=C–H) bend	Methylene group or alkenes group	Strong	873.28	C–H stretching	Aromatics group	Strong
1406.27	(C–C) stretching (ring)	Aromatics group	Medium	1031.37	C–N stretching	Aliphatic amines	Medium
1628.41	N–H bend	1° amines (asymmetric)	Medium	1416.58	C–C Stretching	Aromatics group	Medium
1779.94	C=O Stretching	Anhydrides group **	Strong	2813.81	H–C=O:C–H stretching (or) –COOH	Aldehydes group (or) Carbonyl group	Medium
2794.01	H–C=O:C–H stretching	Aldehydes group	Medium	2882.99	C–H stretching	Alkanes group	Medium
2882.67	C–H stretching	Alkanes	Medium	3276.95	–C≡C–H:C–H stretching (or) O–H stretching	Alkynes (terminal) group or Alcohols groups**	(n—narrow, s—sharp) or (br—broad, s—sharp)
3364.48	N–H stretching	1°, 2° amines and amides	Medium	-	-	-	-

Anhydrides group **— due to the C–O stretch, it absorbs in the fingerprint region.

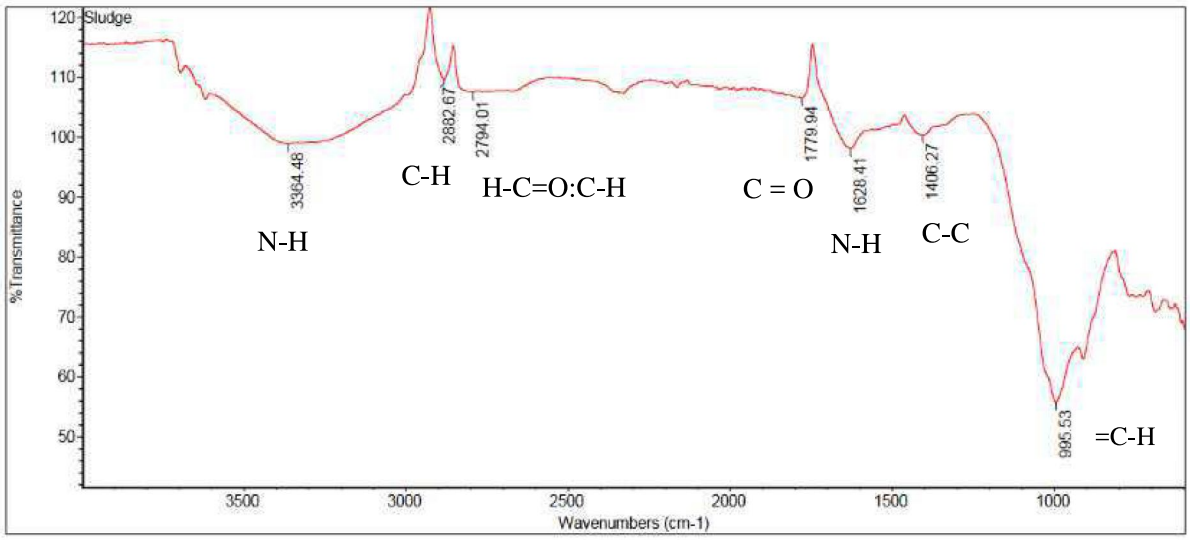

Fig. 5 Fourier transform infrared spectroscopy (FT-IR) analysis reveals the presence of various functional groups in PBS, including = C–H, C–C, N–H, C = O, H–C = O, and C–H

Parameshwari et al. (2018); and Sinha et al. (2020). The broadband at 3364.48 cm^{-1} corresponds to N–H stretching in primary and secondary amines and amides, indicating nitrogen-containing functional groups in the PBS.

The main surface functional groups of biochar are hydroxyl, methyl, carboxylic, and alkene groups as reported by Zhao et al. (2018). Biochar which was pyrolysis under low temperatures (200–400 °C) of biochar has more oxygen-containing functional groups such as –COOH, –OH, C = O, and –CHO) groups which stimulate nutrient exchange and improve soil fertility as reported by Mandal et al. (2021) and Ralebitso-Senior and

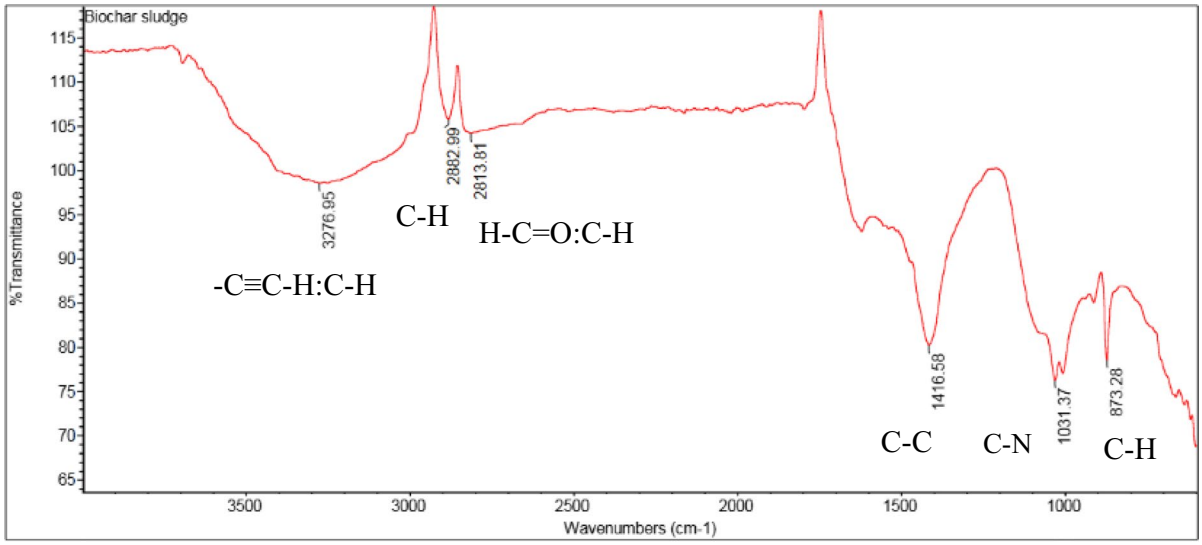

Fig. 6 Fourier Transform Infrared Spectroscopy (FT-IR) analysis reveals the presence of various functional groups in PBSB, including (C-Cl, C-N, C-C, H-C=O: C-H or -COOH or C=O, C-H, and -C≡C-H: C-H or O-H)

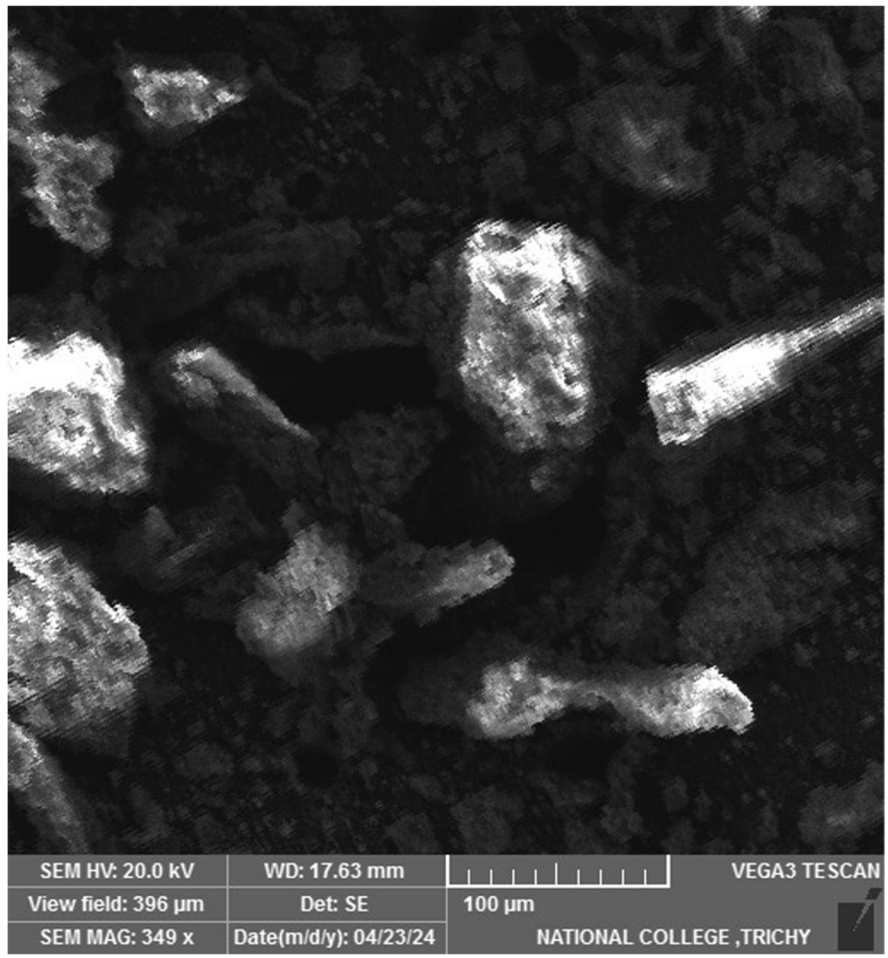

Fig. 7 SEM images of PBS reveal a rough, wrinkled, flaky texture, and a porous structure

Orr (2016). The observed functional groups in PBS biochar (PBSB), such as C–Cl (halo or chloro group), C–N, C–C (aromatic group), H–C = O: C–H (aldehyde group) or –COOH or C = O (carbonyl group), C–H, and –C≡C–H: C–H (alkene group) or O–H (alcohol group) were observed (Fig. 6). The broad band at 850 cm^{-1} in PBS biochar (PBSB) may correspond to C–Cl of alkyl halides with medium intensity, which may enhance biochar's ability to adsorb and retain organic pollutants. Due to the impregnation process, the $CaCO_3$ is transformed into calcium chloride or C–Cl (Manoko et al., 2021). A sharp peak at 873.28 cm^{-1} and 710 cm^{-1} was associated with C–H stretching in aromatic groups with strong intensity and indicating out-of-plane and in-plane bending vibrations of the carbonate ion, which may be derived from the decomposition of cellulose, hemicellulose, and lignin during pyrolysis at relatively low temperatures (≤ 500 °C). A peak at 1031.37 cm^{-1} may correspond to C–N stretching in aliphatic amines; it is formed from nitrogenous biomass components during pyrolysis, and these components change from amine or amide group. It also improves biochar's cation exchange capacity (CEC) and is more effective in nutrient retention (Mohan et al., 2014). C–C stretching in aromatic groups may correspond at 1416.58 cm^{-1} which indicates a more graphitic and stable structure; it increased the stability and may be crucial for long-term carbon sequestration. The strong absorption band was observed around 1440 cm^{-1} and 850 cm^{-1} suggesting the presence of $CaCO_3$, with the band at 1440 cm^{-1} corresponding to asymmetric stretching of the carbonate ion. The broadband at 2813.81 cm^{-1} may correspond to H–C = O:C–H

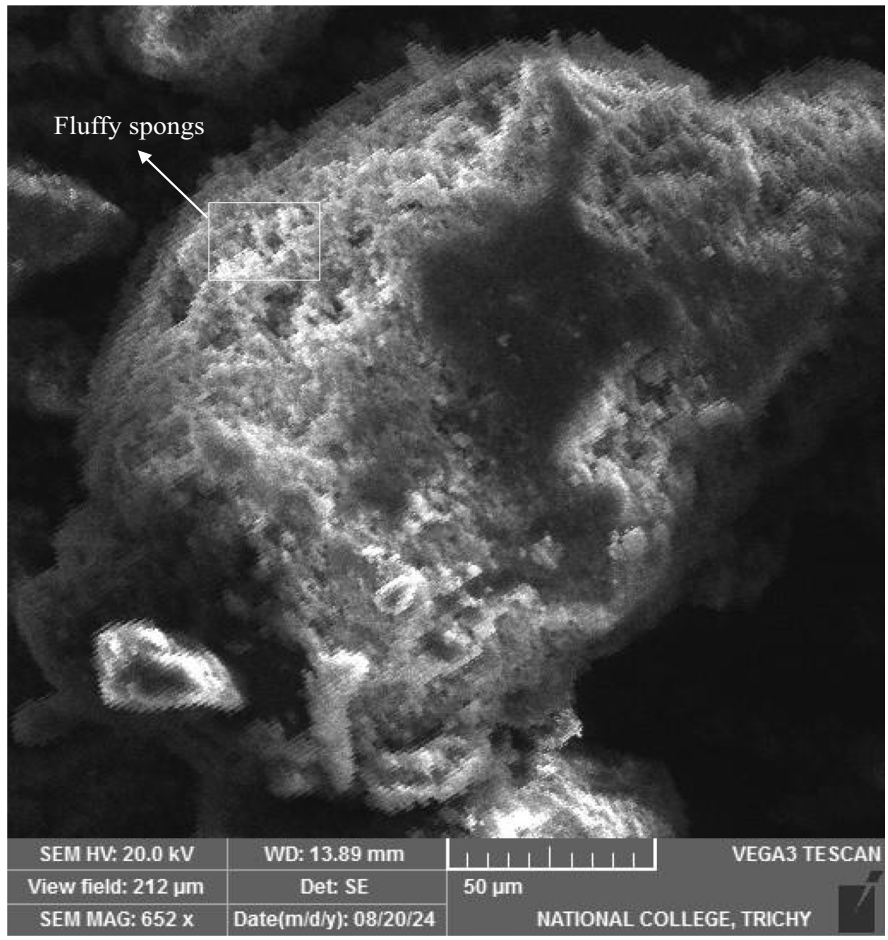

Fig.8 SEM images of PBSB reveal coarse, small cavities, holes, fluffy spongy texture, and a mesoporous structure

Table 4 Elemental analysis of PBS and PBSB collected from Tamil Nadu Paper Limited (TNPL). The K and L following every element indicates the K and L shells of the specific atom

PBS			PBSB		
Element	**Weight%**	**Atomic%**	**Element**	**Weight%**	**Atomic%**
C–K	46.16	56.46	C K	34.46	45.43
O–K	41.53	38.14	O K	45.42	44.95
Na–K	0.42	0.27	Na K	0.33	0.23
Mg–K	0.43	0.26	Mg K	0.41	0.26
Al–K	1.43	0.78	Al K	3.70	2.17
Si–K	2.26	1.18	Si K	3.12	1.76
P–K	0.21	0.10	P K	1.31	0.67
S–K	0.88	0.40	S K	1.42	0.70
Cl–K	0.26	0.11	Cl K	0.38	0.17
K–K	0.24	0.09	K K	0.18	0.07
Ca–K	5.62	2.06	Ca K	8.45	3.34
Fe–K	0.56	0.15	Ti K	0.12	0.04
			Mn K	0.41	0.12
			Fe K	0.30	0.09
Totals	**100.00**		**Totals**	**100.00**	

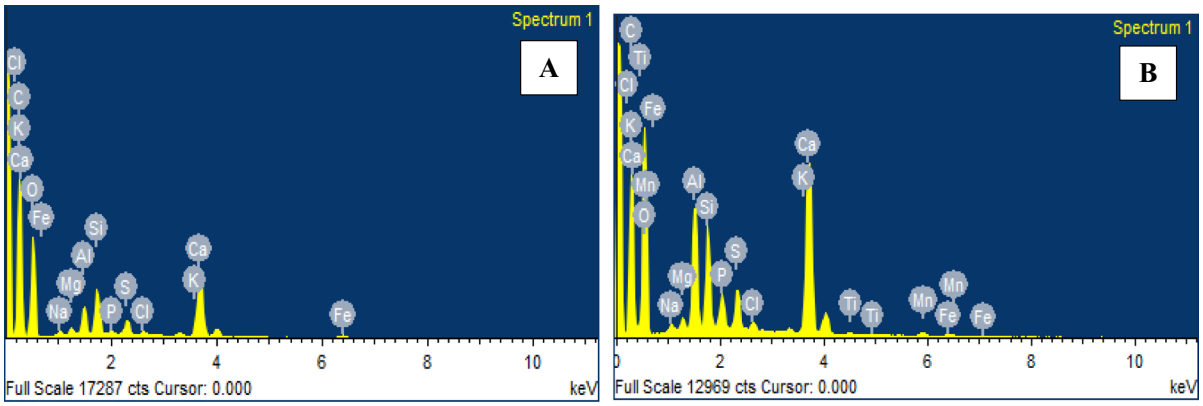

Fig. 9 EDX spectrum reveals the predominately occurred elements of **A** PBS and **B** PBSB

stretching in the aldehydes group with medium intensity, or the –COOH or C = O of the carbonyl group, while the 2882.99 cm^{-1} band corresponds to C–H stretching in the alkanes group. 3276.95 cm^{-1} band may correspond to –C≡C-H:C–H stretching in the alkynes group, which may form under low-oxygen conditions, and suggest unsaturated carbon structures. All the observed bands in PBSB are dependent on the hydration state.

Scanning electron microscopy with energy-dispersive X-ray spectroscopy for PBS and PBSB (SEM–EDX)

The surface structures and morphology of PBS and PBSB were characterized by using scanning electron microscopy (SEM), while their compositions were determined through energy-dispersive X-ray spectroscopy (EDX). The PBS micrograph observations revealed that the sludge surface exhibited a rough, wrinkled, and flaky texture with a porous structure and heterogeneous distribution of particles (Fig. 7). This characteristic makes it possible for the sludge to adsorb metals and various complex organic ions. The mechanism for the adsorption of metal and other complex ions on soil may be physical and chemical adsorption on the surface sites (Yadav & Chandra, 2018). The PBSB micrograph showed that the size reduction of particles was also observed. It has a coarse surface, small cavities, holes, and a (meso and micro) porous structure. Moreover, the surface of PBSB exhibited particle dispersion in the form of fluffy sponges and spherical-shaped particles with deeper fragmentation (Oumabady et al., 2020). The fluffy spongy nature of PBSB is due to the carbon matrix. The fluffy spongy texture and interconnected pores and voids of biochar provide a large surface area and are often attributed to the adsorption of water, nutrients, or pollutants. Due to the low pyrolysis temperature, the PBSB may be hydrophobic in nature (Fig. 8). The pores in biochar play a crucial role in facilitating solid–liquid contact, allowing the passage of pollutants, nutrients, water, or electrolytes to the smaller pores within the biochar's inner structure (Lima et al., 2022; Reis et al., 2022). The fluffy, spongy nature of biochar enhances its ability to improve soil aeration and water retention (Liang et al., 2021). Biochar can become hydrophobic when produced at lower temperatures, which also results in greater structural strength compared to biochar produced at higher temperatures (Nartey & Zhao, 2014).

The energy dispersive X-ray (EDX) spectrum of PBS is shown in Table 4. The predominantly observed element of PBS was carbon (46.16% by weight) and oxygen (41.53% by weight) which may be organic or contain significant amounts of carbonates or oxides. Calcium (5.62% by weight), silicon (2.26% by weight), aluminum (1.43% by weight), and other trace elements were present in the PBS. The Si and Al are indicative of aluminosilicate minerals which are major components of clays like kaolinite ($Al_2Si_2O_5$ $(OH)_4$). These minerals contribute to the structural integrity and CEC of soil. Other trace elements of PBS with individual weight percentages are represented in Table 4.

The energy dispersive X-ray (EDX) spectrum of PBSB is shown in Table 4. The predominantly

observed elements of PBSB were carbon (34.46% by weight) and oxygen (45.42% by weight). Silicon, aluminum, and calcium are present at 3.12%, 3.70%, and 8.45% by weight, respectively. These elements are typically associated with aluminosilicates and carbonates. The presence of silicon and aluminum in biochar indicates aluminosilicate minerals like kaolinite, which are important for maintaining structural integrity and cation exchange capacity (CEC) in both soil and biochar (Wang et al., 2020). Additionally, the phosphorus and potassium in biochar are slowly released into the soil, thereby enhancing nutrient availability (Lehmann & Joseph, 2015). Calcium presence in the form of $CaCO_3$ plays a vital role in regulating soil pH. Fe (0.30%) and Mn (0.41%) are redox-sensitive elements playing a key role in redox reactions within the soil and they undergo oxidation and may trigger the permeability transition pores (PTP). Phosphorus (1.31%) and potassium (0.18%) by weight are essential nutrients in the soil and they may enhance the value of PBS biochar as a slow-release fertilizer. Figure 9)represents the XRD crystalline and amorphous phase of PBS and PBSB.

X-ray diffraction (XRD)

The crystalline and amorphous peak pattern of PBS and PBSB is shown in Table 5. X-ray diffraction was performed to evaluate the PBS properties (Fig. 10). The PBS was observed with some distinct peaks of the more crystalline phase. The strong crystalline peaks observed at 29.6301° 2θ would be attributed to the presence of calcite, which is consistent with that identified the presence of calcium used in the paper production. Calcite is often used in the papermaking process to enhance the brightness and opacity of paper (Reis et al., 2022). The diffraction peak at 44.66° 2θ and 64.84° 2θ can be related to the periclase. The diffraction peaks at 11.7389° 2θ, 20.7562° 2θ, and 31.20° 2θ can suggest the presence of gypsum, a common by-product in paperboard production, particularly in processes that used calcium sulfate. The presence of gypsum in the PBS was expected due to the use of sulfur-containing compounds in the pulping and bleaching processes (Parameshwari et al., 2018). Birnessite and cristobalite were also identified at 42.5348° 2θ and 31.2087° 2θ, respectively. Cristobalite might have formed during high-temperature processes or been present in raw materials containing silica, linked to the use of siliceous

Table 5 X-ray diffraction (XRD) analysis of PBS and PBS biochar

Visible	Ref. code	Score	Compound name	Displ.[°2θ]	Scale Fac	Chem. formula	Ref. code	Score	Compound name	Displ. [°2θ]	Scale Fac	Chem. formula
	96–901–6707	81	Calcite	0.000	1.011	Ca6.00 C6.00 O18.00	96–900–1298	53	Calcite	0.000	0.883	Ca5.62 Mg0.38 C6.00 O18.00
	96–202–1018	37	Digold indium palladium	0.000	0.156	Pd1.37 Au1.77 In0.86	96–901–3220	41	Periclase	0.000	0.140	Mg4.00 O4.00
	96–901–1683	27	Bromargyrite	0.000	0.060	Ag4.00 Br4.00	96–900–1753	36	Gypsum (deuterated)	0.000	0.152	Ca8.00 S8.00 O24.00 D16.00
	96–900–4468	28	Richetite	0.000	0.048	U36.00 Pb8.74 Fe0.47 Mg0.83 O173.00	96–900–1273	24	Birnessite	0.000	0.079	Mn2.00 O5.40 K0.46
	96–900–1754	21	Gypsum (deuterated)	0.000	0.096	Ca8.00 S8.00 O24.00 D16.00	96–900–8229	8	Cristobalite	0.000	0.058	Si4.00 O8.00
	96–500-0209	16	Cerussite	0.000	0.085	Pb4.00 C4.00 O12.00	96–900–9235	22	Kaolinite	0.000	0.074	Al2.00 Si2.00 O9.00 H4.00

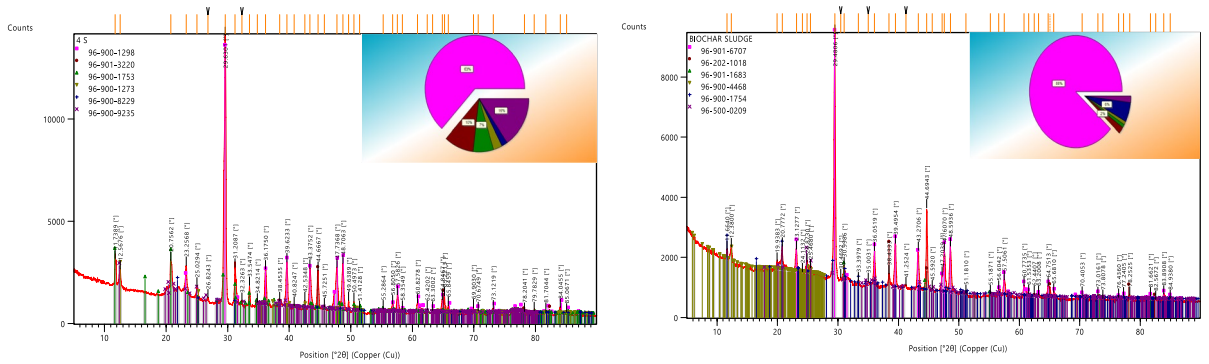

Fig. 10 XRD patterns reveal the crystalline and amorphous phase of PBS and PBSB

materials in the paper production process. The peak at 12.5676° 2θ indicated the presence of kaolinite, which was frequently used in the paper industry as a filler and coating material. Kaolinite contributed to the mineralogical composition of the sludge due to its abundance in the raw materials and its stability during processing (Harmsen & Naidu, 2013).

X-ray diffraction (XRD) was performed to evaluate the PBSB properties (Fig. 10). The PBSB was observed with some distinct peaks of the more crystalline phase. The strong crystalline peaks observed at 29.4806° 2θ, 23.1277° 2θ, and 39.4954° 2θ were attributed to the presence of calcite, which indicates the presence of calcium carbonate used in paper production processes and may be used as fillers or pigments. During the pyrolysis process, calcite can persist as a stable, because of its resistance at low temperatures. The diffraction peaks were observed at 38.433° 2θ, 44.6943° 2θ, and 8.2525° 2θ indicating the presence of digold indium palladium. Bromargyrite and Richetite were also observed at the peak of 30.9986° 2θ, 12.3800° 2θ, and 24.1132° 2θ, respectively. The amorphous peak was observed at 6640° 2θ, 20.7772° 2θ, 51.1810° 2θ, and 55.1871° 2θ indicating the presence of gypsum (deuterated), and cerusite is identified at the peak of 19.9383° 2θ, 24.8730° 2θ, 25.4680° 2θ, 35.0031° 2θ, and 41.2524° 2θ.

Conclusion

This study highlights the potential of converting PBS into biochar through slow pyrolysis, significantly altering its physicochemical properties. In general, PBSB has high organic carbon, fixed carbon, TOC, carbonates, and aluminosilicates which were further confirmed by FT-IR spectroscopy and SEM–EDX analyses. FT-IR analysis of PBSB identified the presence of various carbon-containing functional groups, including C–Cl, C–N, C–C, H–C=O, C–H, and –C≡C–H, indicating substantial chemical transformations during pyrolysis. The TGA analysis of the dried paperboard sludge sample showed a 20% mass reduction when heated to 350 °C. During this process, more than 90% of the volatile components were removed. SEM–EDX analysis revealed that PBSB has fine particle size and a coarse fluffy spongy porous structure ideal for water adsorption. Elemental analysis (XRD) showed high carbon and oxygen content with significant amounts of aluminosilicates, carbonates, and nutrients like phosphorus, potassium, iron, manganese, copper, and zinc suggesting PBSB as a potential slow-release fertilizer.

Acknowledgements The authors express their sincere gratitude to TNPL Unit – II for their generous support and the instrumental facilities provided by the TNAU, Centre of Excellence in Sustaining Soil Health, ADAC&RI, Tiruchirappalli and National College Instrumentation Facility, Tiruchirappalli. Special thanks to Dr.R.K.Kaleeswari, Project Director, CoE-SSH, TNAU, Tiruchirappalli for rendering invaluable assistance in instrumental facilities.

Author contribution All authors have made substantial contributions to the conception, design, analysis, and interpretation of data for the work. Sherene Jenita Rajammal and Vaishnavi Pandurugan contributed to analytical part, drafting the manuscript and revising it critically for important intellectual content. The authors Baskar Murugaiyan and Vanniarajan Chokalingam contributed final drafting of the manuscript and Ramjani S A helped in preparing sludge biochar and proximate

analysis. All the authors gave final approval for the version to be published and agreed to be accountable for all aspects of the work in ensuring that questions related to the accuracy or integrity of any part of the work are appropriately investigated and resolved.

Data availability No datasets were generated or analysed during the current study.

Declarations

Ethics approval This research is entirely original, with no content copied from other sources. All ideas and work from others have been properly cited. The results are reported honestly, without any fabrication or manipulation of data. Additionally, the study's limitations are transparently explained. Only individuals who have made significant contributions to the research are listed as authors, and all authors have reviewed and approved the final version of the manuscript before submission.

Conflict of interest The authors declare no competing interests.

References

Agrafioti, E., Bouras, G., Kalderis, D., & Diamadopoulos, E. (2013). Biochar production by sewage sludge pyrolysis. *Journal of Analytical and Applied Pyrolysis, 101*, 72–78.

American Public Health Association. (1926). Standard methods for the examination of water and wastewater (Vol. 6). American Public Health Association.

ASTM D2216–98. Standard test method for laboratory determination of water (moisture). Content of Soil and Rock by Mass USA; 2005.

Bajpai, P. (2015). *Management of pulp and paper mill waste* (Vol. 431). Springer International Publishing.

Bolan, N. S., Kunhikrishnan, A., Choppala, G. K., Thangarajan, R., & Chung, J. W. (2012). Stabilization of carbon in composts and biochars in relation to carbon sequestration and soil fertility. *Science of the Total Environment, 424*, 264–270.

dos Reis, G. S., Guy, M., Mathieu, M., Jebrane, M., Lima, E. C., Thyrel, M., ... & Larsson, S. H. (2022). A comparative study of chemical treatment by MgCl2, ZnSO4, ZnCl2, and KOH on physicochemical properties and acetaminophen adsorption performance of biobased porous materials from tree bark residues. *Colloids and Surfaces A: Physicochemical and Engineering Aspects*, *642*, 128626.

Faubert, P., Barnabé, S., Bouchard, S., Côté, R., & Villeneuve, C. (2016). Pulp and paper mill sludge management practices: What are the challenges to assess the impacts on greenhouse gas emissions? *Resources, Conservation and Recycling, 108*, 107–133.

Ferreira, C. I., Calisto, V., Cuerda-Correa, E. M., Otero, M., Nadais, H., & Esteves, V. I. (2016). Comparative valorisation of agricultural and industrial biowastes by combustion and pyrolysis. *Bioresource Technology, 218*, 918–925.

Geyer, R., Jambeck, J. R., & Law, K. L. (2017). Production, use, and fate of all plastics ever made. *Science Advances, 3*(7), e1700782.

Guo, M. (2020). The 3R principles for applying biochar to improve soil health. *Soil Systems, 4*(1), 9.

Harmsen, J., & Naidu, R. (2013). Bioavailability as a tool in site management. *Journal of Hazardous Materials, 261*, 840–846.

Harvey, O. R., Kuo, L. J., Zimmerman, A. R., Louchouarn, P., Amonette, J. E., & Herbert, B. E. (2012). An index-based approach to assessing recalcitrance and soil carbon sequestration potential of engineered black carbons (biochars). *Environmental Science & Technology, 46*(3), 1415–1421.

Holladay, J. E., White, J. F., Bozell, J. J., & Johnson, D. (2007). *Top value added chemicals from biomass-volume II, Results of screening for potential candidates from biorefinery lignin* (No. PNNL-16983). Pacific Northwest National Laboratory (PNNL), Richland, WA (United States); National Renewable Energy Laboratory (NREL), Golden, CO (United States).

Hossain, M. K., Strezov, V., Chan, K. Y., Ziolkowski, A., & Nelson, P. F. (2011). Influence of pyrolysis temperature on production and nutrient properties of wastewater sludge biochar. *Journal of Environmental Management, 92*(1), 223–228.

Jaria, G., Silva, C. P., Ferreira, C. I., Otero, M., & Calisto, V. (2017). Sludge from paper mill effluent treatment as raw material to produce carbon adsorbents: An alternative waste management strategy. *Journal of Environmental Management, 188*, 203–211.

Joseph, S. D., Camps-Arbestain, M., Lin, Y., Munroe, P., Chia, C. H., Hook, J., ... & Amonette, J. E. (2010). An investigation into the reactions of biochar in soil. *Soil Research*, *48*(7), 501–515.

Junior, A., & Guo, M. (2023). Efficacy of sewage sludge derived biochar on enhancing soil health and crop productivity in strongly acidic soil. *Frontiers in Soil Science, 3*, 1066547.

Kambo, H. S., & Dutta, A. (2015). A comparative review of biochar and hydrochar in terms of production, physicochemical properties and applications. *Renewable and Sustainable Energy Reviews, 45*, 359–378.

Kumar, M., & Chopra, R. (2015). Utilization of mulling oils in paperboard manufacturing. *International Journal of Paper Science., 7*(3), 112–118.

Lehmann, J., & Joseph, S. (2015). Biochar for environmental management: An introduction. In *Biochar for Environmental Management* (pp. 1–13). Routledge.

Liang, J., Chen, Y., Cai, M., Gan, M., & Zhu, J. (2021). One-pot pyrolysis of metal-embedded biochar derived from invasive plant for efficient Cr (VI) removal. *Journal of Environmental Chemical Engineering, 9*(4), 105714.

Likon, M., & Trebše, P. (2012). Recent advances in paper mill sludge management. *Industrial Waste*, 73–90.

Lima, R. M. A. P., Dos Reis, G. S., Thyrel, M., Alcaraz-Espinoza, J. J., Larsson, S. H., & de Oliveira, H. P. (2022). Facile synthesis of sustainable biomass-derived porous biochars as promising electrode materials for

high-performance supercapacitor applications. *Nanomaterials, 12*(5), 866.

Mandal, S., Pu, S., Adhikari, S., Ma, H., Kim, D. H., Bai, Y., & Hou, D. (2021). Progress and future prospects in biochar composites: Application and reflection in the soil environment. *Critical Reviews in Environmental Science and Technology, 51*(3), 219–271.

Manoko, M. C., Chirwa, E. M., & Makgopa, K. (2021). Structural elucidation of magnetic biochar derived from recycled paper waste sludge. *Chemical Engineering Transactions, 88*, 193–198.

Manyà, J. J. (2012). Pyrolysis for biochar purposes: A review to establish current knowledge gaps and research needs. *Environmental Science & Technology, 46*(15), 7939–7954.

Méndez, A., Fidalgo, J. M., Guerrero, F., & Gascó, G. (2009). Characterization and pyrolysis behaviour of different paper mill waste materials. *Journal of Analytical and Applied Pyrolysis, 86*(1), 66–73.

Mohan, D., Sarswat, A., Ok, Y. S., & Pittman, C. U., Jr. (2014). Organic and inorganic contaminants removal from water with biochar, a renewable, low cost and sustainable adsorbent–a critical review. *Bioresource Technology, 160*, 191–202.

Nartey, O. D., & Zhao, B. (2014). Biochar preparation, characterization, and adsorptive capacity and its effect on bioavailability of contaminants: An overview. *Advances in Materials Science and Engineering, 2014*(1), 715398.

Nelson, D. W., & Sommers, L. E. (1982). Total carbon, organic carbon, and organic matter. *Methods of Soil Analysis: Part 2 Chemical and Microbiological Properties, 9*, 539–579.

Oumabady, S., Kamaludeen, S. P., Ramasamy, M., Kalaiselvi, P., & Parameswari, E. (2020). Preparation and characterization of optimized hydrochar from paper board mill sludge. *Scientific Reports, 10*(1), 773.

Parameshwari, R., Gopalakrishnan, S., & Sinha, P. (2018). Effect of coating formulations on paperboard properties. *Journal of Applied Polymer Science., 135*(22), 46323.

Ralebitso-Senior, T. K., & Orr, C. H. (2016). Microbial ecology analysis of biochar-augmented soils: Setting the scene. In *Biochar application* (pp. 1–40). Elsevier.

Sabarish, K., Sebastian, S. P., Maheswari, M., Balasubramaniam, P., & Ejilane, J. (2021). Production and characterization of paper board mill ETP sludge derived hydrochar. *International Journal of Environment and Climate Change, 11*(11), 1–8.

Simões Dos Reis, G., Bergna, D., Tuomikoski, S., Grimm, A., Lima, E. C., Thyrel, M., ... & Larsson, S. H. (2022). Preparation and characterization of pulp and paper mill sludge-activated biochars using alkaline activation: A box–Behnken design approach. *ACS Omega*, *7*(36), 32620–32630.

Sinha, P., Gopalakrishnan, S., & Parameshwari, R. (2020). Optimization of pigment dispersion in paperboard coatings. *Materials Today: Proceedings., 21*, 2042–2047.

Tawalbeh, M., Rajangam, A. S., Salameh, T., Al-Othman, A., & Alkasrawi, M. (2021). Characterization of paper mill sludge as a renewable feedstock for sustainable hydrogen and biofuels production. *International Journal of Hydrogen Energy, 46*(6), 4761–4775.

Turner, T., Wheeler, R., & Oliver, I. W. (2022). Evaluating land application of pulp and paper mill sludge: A review. *Journal of Environmental Management, 317*, 115439.

Venkatesh, G., Gopinath, K. A., Reddy, K. S., Reddy, B. S., Prabhakar, M., Srinivasarao, C., ... & Singh, V. K. (2022). Characterization of biochar derived from crop residues for soil amendment, carbon sequestration and energy use. *Sustainability*, *14*(4), 2295.

Wang, Y., Zhang, K., Lu, L., Xiao, X., & Chen, B. (2020). Novel insights into effects of silicon-rich biochar (Sichar) amendment on cadmium uptake, translocation and accumulation in rice plants. *Environmental Pollution, 265*, 114772.

Yadav, S., & Chandra, R. (2018). Detection and assessment of the phytotoxicity of residual organic pollutants in sediment contaminated with pulp and paper mill effluent. *Environmental Monitoring and Assessment, 190*(10), 581.

Yang, F., Zhao, L., Gao, B., Xu, X., & Cao, X. (2016). The interfacial behavior between biochar and soil minerals and its effect on biochar stability. *Environmental Science & Technology, 50*(5), 2264–2271.

Zhao, Y., Zhao, L., Mei, Y., Li, F., & Cao, X. (2018). Release of nutrients and heavy metals from biochar-amended soil under environmentally relevant conditions. *Environmental Science and Pollution Research, 25*, 2517–2527.